Comparative study of the electronic structure of MgB_2 and ZrB_2

C. Jariwala,[1,*] A. Chainani,[1] S. Tsuda,[2] T. Yokoya,[2] S. Shin,[2,3] Y. Takano,[4] K. Togano,[4] S. Otani,[4] and H. Kito[5]
[1]*Institute for Plasma Research, Bhat, Gandhinagar 382 428, India*
[2]*Institute for Solid State Physics, University of Tokyo, Kashiwa, Chiba 277-8581, Japan*
[3]*The Institute of Physical and Chemical Research (RIKEN), Sayo-gun, Hyogo 679-5143, Japan*
[4]*National Institute for Materials Science, Tsukuba, Ibaraki 305-0047, Japan*
[5]*National Institute of Advanced Industrial Science and Technology, Umezono, Tsukuba 305-8568, Japan*
(Received 5 June 2003; revised manuscript received 29 August 2003; published 6 November 2003)

X-ray photoemission spectroscopy is used to compare the electronic structures of MgB_2 and ZrB_2. The B 1*s* core levels in high-quality MgB_2 and ZrB_2 exhibit a single asymmetric peak typical of a metallic boride. The Mg 2*p* core level shows a single peak with negligible intensity in charge-transfer satellites and no correlation effects. The Mg 2*p* and B 1*s* core-level spectra exhibit a broad bulk plasmon feature centered at about 22 eV from the main peak, in good accord with calculations. The measured valence bands are consistent with band-structure calculations indicating a higher density of states (DOS) at E_F for MgB_2 compared to ZrB_2. The high T_c in MgB_2 is due to *p*-derived DOS, while ZrB_2 is dominated by *d*-derived states at E_F.

DOI: 10.1103/PhysRevB.68.174506 PACS number(s): 74.25.Jb, 74.25.Kc, 79.60.Bm

The unexpected discovery of superconductivity in MgB_2 with a transition temperature $T_c = 39$ K,[1] the highest T_c in intermetallic compounds, has created a sensation in the solid-state community. The T_c of MgB_2 being slightly higher than the upper limit known for conventional phonon-mediated superconductivity,[2,3] some studies have concluded that superconductivity in this layered material is nonconventional.[4] Similarities and dissimilarities with conventional superconductors and the high-T_c cuprates have invariably been invoked.[5]

MgB_2 possesses the simple hexagonal AlB_2-type structure (space group $P6/mmm$) and is a common structure for many metal diborides including TaB_2, ZrB_2, etc.[6] It consists of hexagonal close-packed graphitelike boron layers separated by metal ion layers. Its simple structure makes it more interesting to unravel its superconductivity. Boron isotope effect[7] and Boron NMR[8] studies suggest that MgB_2 is a conventional phonon-mediated *s*-wave superconductor. The measured phonon density of states (DOS) in MgB_2 extends up to a high value of ~ 100 meV.[9] Band-structure calculations do show that MgB_2 has a high DOS at E_F, $N(E_F)$ consisting primarily of B $2p_\sigma$ states.[10–14] Recent angle-resolved photoemission spectroscopy (ARPES) measurements[15] conclude that electron-electron correlations are weak by comparing with band-structure calculations and support a conventional pairing mechanism in MgB_2. The ARPES study, however, does not rule out the renormalization of the electronic structure on phonon energy scales and points out the role of multiple bands to account for properties of MgB_2, such as the Hall coefficient.[16] Superconducting gap measurements from tunneling conductance[17] and high-resolution ultraviolet photoemission spectroscopy (UPS) (Ref. 18) show a multiple gap suggestive of a pairing mechanism involving different Fermi surfaces. Heat-capacity measurements on single crystal MgB_2 also conclude two-band superconductivity with a small isotropic and a large anisotropic gap.[19] The two-band model,[20,21] with differing gaps on different Fermi surface sheets, is a strong candidate for explaining properties of MgB_2. The multiple gap behavior from tunneling, UPS, and heat-capacity studies with a $2\Delta/k_BT_c > 3.5$ for a large gap and $2\Delta/k_BT_c < 3.5$ for the small gap is indeed very different.

In this work, we study the electronic structure of MgB_2 and compare it with ZrB_2 using x-ray photoemission spectroscopy (XPS). We chose to compare ZrB_2 with MgB_2, as ZrB_2 is closest to MgB_2 structurally ($c/a = 1.115$ and 1.142, respectively, Ref. 6). ZrB_2 has also been reported to be a superconductor with a $T_c = 5.5$ K,[22] but other studies[23] and single crystals used in the present study did not show superconductivity down to 2 K. While XPS studies have been reported for MgB_2, Vasquez *et al.*[24] and Ueda *et al.*[25] report a weak B_2O_3 feature along with the MgB_2 B 1*s* signal. Their Mg 2*p* core-level spectra also exhibit two features, out of which only one is intrinsic to MgB_2. A theoretical study has compared available experimental data with cluster calculations and conclude that MgB_2 should exhibit charge-transfer (CT) satellites in Mg 2*p* XPS spectra, implying strong correlation effects.[26] A recent photoemission microscopy study using synchrotron radiation reports a single peak Mg 2*p* core level, but the B 1*s* core level shows multiple loss features within 6 eV of the main peak.[27] The authors interpret the loss features as originating from low-energy plasmons at 2.6 and 5.0 eV, and dipole allowed transitions at 1.55 and 3.65 eV from the main peak. While the valence-band spectra of Ref. 27 show consistency with band-structure calculations only when they measure at submicron resolution on a single grain, the core-level spectra they report are in the conventional mode and integrated over an area encompassing many grains. They themselves show that the valence band in the two cases are different, and hence the core-level spectra cannot be reliable. Most importantly, they also use the same technique as ours for surface cleaning, but contrary to earlier reports as well as ours, theirs is the only study which reports loss features in the B 1*s* core level in addition to the main peak. The loss features observed by them in the B 1*s* spectrum lead to a serious issue of interpretation of core-level features, as they attribute it to plasmon or collective excita-

tions. This is clearly incorrect, simply because if that be the case, the Mg $2p$ core level should also show the same loss features. In their own data, the Mg $2p$ spectrum does not show the same loss features. Hence, the data presented by them for the core-level spectra only lead to further confusion in the literature. In order to check these features as well as the bulk plasmon excitation in MgB_2, we have carried out high signal-to-noise ratio measurements of the B $1s$ and Mg $2p$ core levels. We show that the interpretation of Vasquez *et al.* is correct regarding the Mg $2p$ peak and that MgB_2 does not show CT satellites. The intrinsic Mg $2p$ and B $1s$ core levels are single peaks and their line shape is best explained as an asymmetric Doniach-Sunjic (DS) line shape due to its metallicity. In addition, the bulk plasmon satellite is observed at about 22 eV from the main peak as a broad feature in the B $1s$ and Mg $2p$ core levels, confirming the calculations.[28] We also report the core-level and valence-band spectra comparison between MgB_2 and ZrB_2. The valence bands are consistent with band-structure calculations and the relative intensity at E_F indicates a much higher DOS at E_F for MgB_2 compared to ZrB_2.

High quality samples of polycrystalline MgB_2 and single crystal ZrB_2 were synthesized and characterized as reported recently.[29] MgB_2 showed a T_c onset of 38 K with a transition width of 1.5 K, while ZrB_2 showed no superconductivity down to 2 K.[29] XPS spectra were obtained using a Multitechnique Physical Electronics System 5702, Minnesota, U.S.A. The base vacuum was 8.0×10^{-10} torr and all measurements were done at room temperature with a very high signal-to-noise ratio. A monochromatic Al $K\alpha$ ($h\nu=1486.6$ eV) photon source was used with a pass energy of 11.75 eV for a total resolution of 0.57 eV full width at half maximum (FWHM) for the Ag $3d_{5/2}$ peak. The binding-energy scale was calibrated with the Ag $3d_{5/2}$ peak at 368.29 ± 0.05 eV. The samples were cleaned *in situ* by Ar ion etching with the gun operating at 5 keV and a vacuum of 6×10^{-9} torr. Ar ion etching at 500 eV was used recently[27] for MgB_2, and they report a Mg:B ratio close to 1:2. At 500 eV the preferential sputtering is expected to be higher than at 5 keV,[30] while at 5 keV the surface is expected to be more disordered or damaged. We confirmed that etching at 5 keV yields data nearly identical to the 500-eV etched data measured on the same samples (Fig. 1). However, Ar ion etching is known to often damage the surface morphology and electronic structure, and can also cause amorphization even at energies of 500–1000 eV. For example, for a Si-SiO_2 interface, Ar ion etching at 500 eV causes ion knock-on mixing,[31] while for single-crystal metal surfaces of Au(110) and Cu(111), Ar ion etching at 600 and 1000 eV causes morphological changes and dislocation pits on the surface, respectively.[32,33] Ion irradiation with 1000 eV Ar ions leads to amorphization of polycrystalline chemical vapor deposited diamond films.[34] For InP(110), ion etching leads to damage which can be explained as due to a subsurface nucleation of amorphous regions.[35] Also, GaN etched with an Ar plasma at an applied substrate bias of 150–400 eV leads to preferential sputtering and damage which changes the electrical properties of the material.[36] In our case, etching with 500 and 5 KeV Ar ions yields core-level data with a peak width larger than the chemically etched surface (Ref. 24), suggesting that the surface is suboptimal due to etch damage compared to the chemically etched surface, but the core-level spectra in the present case are free of contamination features. Most importantly, the valence bands for MgB_2 and ZrB_2 are measured to be consistent with band-structure calculations,[10–14] indicating that the surface is not amorphous and the spectra represent the intrinsic crystalline electronic structure. The valence-band spectrum of MgB_2 is consistent with the work of Ref. 27 using photoemission microscopy of a single crystalline grain with the surface cleaned by 500-eV Ar ion etching, but in contrast to the valence-band spectrum obtained from a chemically etched surface (Ref. 24). Further, we could obtain contamination free data in the correct concentration ratio of 1:2, with Mg $2p$ and B $1s$ peak widths comparable or narrower than in Ref. 27. The peak FWHM for B $1s$ core level is 1.5 or 1.55 eV in our case and 1.6 eV in Ref. 27, while the Mg $2p$ data are significantly narrower in our case: 1.44 eV, compared to 1.90 eV in Ref. 27. The O $1s$ and C $1s$ concentration on the surface was less than 1% at the start of data collection. The measurement was stopped after 2 h for a 10 min etching when the concentration of O $1s$ reached to 3%.

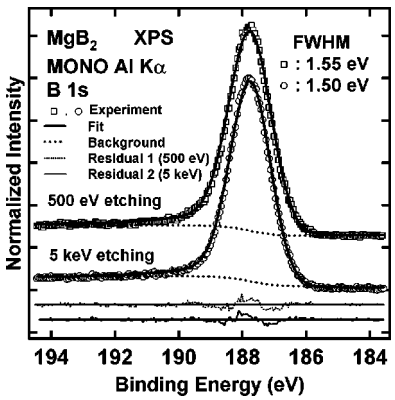

FIG. 1. The Boron $1s$ core-level XPS spectrum of MgB_2 obtained using a monochromatic Al $K\alpha$ source ($h\nu=1486.6$ eV). The thick line superimposed on the data is the best fit Doniach-Sunjic line shape to the spectrum.

Figure 1 shows the B $1s$ core level XPS spectra of MgB_2 obtained using a monochromatic Al $K\alpha$ source, for 500-eV and 5-keV etched surfaces. The spectrum is a single peak in both cases with nearly identical widths (1.55 eV at 500 eV and 1.50 eV at 5 KeV), occurring at a binding energy (BE) of 187.82 eV. This binding energy is typical of a metallic boride and confirms the high quality of the surface. This is in contrast to spectra reported recently for MgB_2 surfaces, which show an extra B_2O_3 feature at 192-eV BE (Refs. 24 and 25) or multiple (four) loss features within 6 eV of the main peak.[27] We could fit a single asymmetric DS line shape (superimposed as a thick line in Fig. 1) with a FWHM 1.50 ± 0.05 eV to the B $1s$ core level. The excellent fit to a single asymmetric peak is evident from Fig. 1, indicative of the metallic nature of the spectrum. The peak width is larger than that reported for the main peak by Vasquez *et al.*[24] for chemically etched surfaces, but slightly narrower than that of Ueda *et al.*,[25] (who measured as grown *in situ* deposited thin film

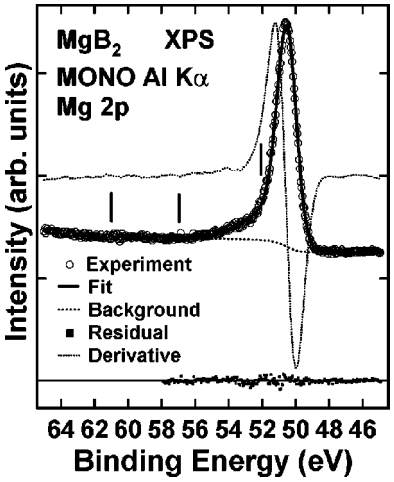

FIG. 2. The Mg $2p$ core-level XPS spectrum of MgB_2 obtained using a monochromatic Al $K\alpha$ source ($h\nu = 1486.6$ eV). The superimposed line is a Doniach-Sunjic line shape and the vertical tick marks indicate charge-transfer satellite positions as calculated in Ref. 26. The derivative spectrum shows negligible satellite intensity.

surfaces) and Goldoni *et al.*[27] (who used Ar ion etching at 500 eV).

In Fig. 2 we report the Mg $2p$ core-level spectrum of MgB_2 using a monochromatic Al $K\alpha$ source. The Mg $2p$ spectrum is also a single peak positioned at 50.54 eV BE (FWHM = 1.44 eV) in contrast to data reported recently. We also plot a derivative of the spectrum to show negligible intensity in the charge-transfer satellites. Vasquez *et al.* reported a main peak at 49.35 eV, with a weak feature at 51.3 eV. But they correctly interpreted the weak feature as of contamination origin. Ueda *et al.* reported a very broad peak with maximum intensity at 49.5 eV and a shoulder at lower binding energy but do not discuss its origin. Although the binding energies reported here are not the same as reported earlier, an important point to note is that the separation between the B $1s$ and Mg $2p$ core levels is 137.28 eV from our data and 137.20 eV from the data of Vasquez *et al.*, indicating good reproducibility for the relative energy scale. In a very recent analysis, Dobrodey *et al.*[26] report cluster calculations of the Mg $2p$ core-level spectrum and conclude that MgB_2 should exhibit intense satellites caused by a $2p_{x,y} \rightarrow$Mg $3s,3p$ CT. They imply that the higher BE feature in the data of Vasquez *et al.* is intrinsic to MgB_2. Further, their calculations for a Mg_2B_4 cluster show high intensity in satellites at $\sim$2 eV, 6 eV, and 10 eV (labeled *A*, *B*, and *C* in Ref. 26, and indicated as vertical tick marks in Fig. 2). The present data indicates negligible intensity in the satellites, while the main peak shows an asymmetry which can be fitted well using a single DS line shape (shown as a thick line). A curve fit to the spectrum using two peaks with a fixed energy separation as calculated by Dobrodey *et al.* resulted in a larger residual. A constraint-free two peak fit showed 1.25% intensity in the satellite peak at 3.17 eV, and no evidence for satellites at 6 or 10 eV from the main peak. From this analysis, we conclude that MgB_2 shows negligible intensity in satellites of the Mg $2p$ core levels and hence no correlation

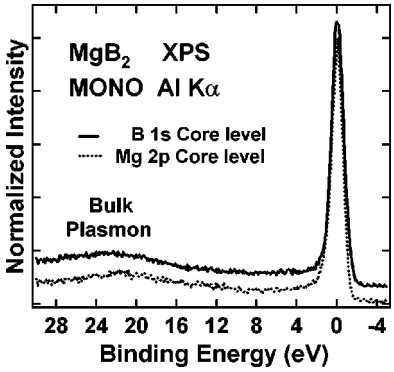

FIG. 3. The Boron $1s$ and Mg $2p$ core-level XPS spectrum of MgB_2 obtained using a monochromatic Al $K\alpha$ source ($h\nu = 1486.6$ eV). The spectra plotted on a common energy scale with the main peak at zero eV show a common broad feature due to the bulk plasmon centered about 22 eV from the main peak.

effects. However, the Mg $2p$ and B $1s$ core levels measured up to high binding energy above the main peak show a clear common feature of the bulk plasmon feature in both the core levels. In Fig. 3, we plot the Mg $2p$ and B $1s$ core-level spectra on a common energy scale with the main peak at zero eV. The data show a broad feature centered at about 22 eV above the main peak, in good accord with the bulk calculated plasmon loss feature[28] and the electron energy loss spectrum of MgB_2.[37] This confirms that the data presented here represent the intrinsic bulk character of the electronic structure. The present study shows no evidence for low-energy loss features, in contrast to the synchrotron study of Ref. 27 which reported loss features only in the B $1s$ core-level spectra.

The XPS spectra for B $1s$ and Zr $3d$ core-levels of ZrB_2 are shown in Fig. 4. The B $1s$ spectrum is a single peak at a binding energy of 187.81 eV (FWHM = 1.34 eV), very similar to that of MgB_2 (187.82 eV). The Zr $3d$ levels consist of the spin-orbit split $3d_{5/2}$ and $3d_{3/2}$ in the correct intensity ratio (3:2) and are also single asymmetric peaks at a binding energy of 178.89 and 181.30 eV, respectively. The best fit using DS line shapes is shown superimposed on the data.

Figure 5 shows the valence-band spectra of MgB_2 com-

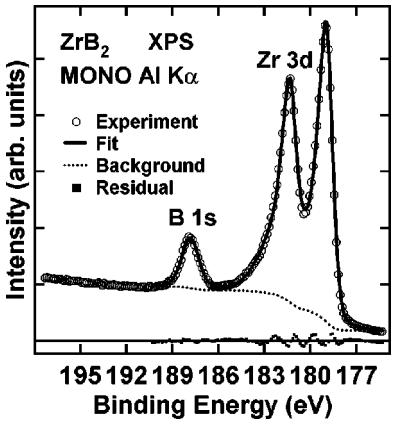

FIG. 4. The Boron $1s$ and Zr $3d_{3/2}$ and $3d_{5/2}$ core-levels in ZrB_2 obtained using a monochromatic Al $K\alpha$ source ($h\nu = 1486.6$ eV).

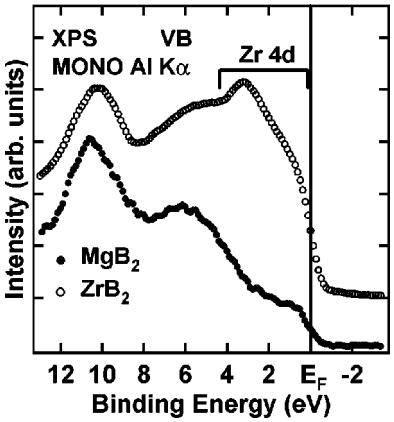

FIG. 5. The valence-band spectra of MgB_2 and ZrB_2 obtained using a monochromatic Al $K\alpha$ source ($h\nu=1486.6$ eV). A Fermi edge is measured in both cases and the Zr $4d$ states are clearly identified.

pared with ZrB_2 and both the spectra show a clear Fermi edge and common features over large energy scales. In particular, comparing with band-structure calculations[10–14] the feature at 8–12 eV binding energy is due to the B $2s$ derived states and is observed for MgB_2 and ZrB_2. Note that B $2s$ has a much higher ($\sim$100 times) atomic cross section than that of B $2p$ at $h\nu=1486.6$ eV,[38] and hence B $2s$ feature shows higher intensity, though the B $2s$ DOS is less than B $2p$. The data are consistent with B K edge ($1s$) x-ray emission studies,[39] which pick up only the p derived states in the valence band. The broad feature at 5–8 eV is also similar in both compounds and is due to predominantly B $2p_\sigma$ and $2p_\pi$ states. While B $2p_\sigma$ and $2p_\pi$ states also contribute to the feature in MgB_2 at and near E_F (Refs. 10–14) the intensity at and within 4 eV of E_F for ZrB_2 is dominated by Zr $4d$ derived states.[12,13] The valence bands of both MgB_2 and ZrB_2 are thus well explained by band-structure calculations. Other probes of electronic structure such as x-ray emission and absorption spectroscopy[37,39] which probe site-selective orbital-angular momentum projected DOS, as well as ARPES,[15] also concluded that the valence band of MgB_2 is consistent with the band-structure calculations. An early XPS study of ZrB_2 (Ref. 40), also concluded consistency with band structure calculations. However, in the earlier study, spectral features due to ZrO_2 in the valence band and core-levels were artificially removed from the observed spectra. In the present work, we find no evidence of ZrO_2 in the core-levels and the valence band. The spectrum is thus of a high quality and represents the intrinsic valence band of ZrB_2. In particular, the clear feature due to the $4d_{xz,yz}$ dominated peak at 3.4 eV and the $4d_{xy,x^2-y^2}$ dominated shoulder at lower binding energies up to E_F is very consistent with the calculations of Rosner *et al.*[13]

The relative intensity at E_F is three times higher in ZrB_2 compared to MgB_2 when we normalize the spectra at the B $2s$ dominated peak at 10.4 eV in Fig. 4. The calculated $N(E_F)$ for ZrB_2 is actually smaller than that for MgB_2 [$N(E_F)=0.16$–0.26 states/eV, cell for ZrB_2, and $N(E_F)=0.72$–0.75 states/eV, cell for MgB_2 (Refs. 10–14)]. This may seem to be in contrast with the data reported here but the intensity at E_F for ZrB_2 consists primarily of Zr $4d$ states and is higher simply due to the much higher ($\sim$450 times) atomic cross section of Zr $4d$ compared to B $2p$ states when using XPS.[38] The calculated values of $N(E_F)$ due to B $2p$ derived states are about 15 times less than the total $N(E_F)$ in MgB_2 (Refs. 10–14). If we assume atomic cross sections, it implies that more than 98% of the intensity at E_F in ZrB_2 is due to Zr $4d$ states and that the experimentally measured relative $N(E_F)$ is very low for ZrB_2 compared to MgB_2. Alternatively, the relative $N(E_F)$ is very high for MgB_2 compared to ZrB_2. While the present study can only make a relative comparison and we cannot obtain the absolute $N(E_F)$, Hall-coefficient studies indicate a very high carrier concentration of 1.7–2.8×10^{23} at 300 K[16] for MgB_2. In this context, it is important to note that the two-band model shows better agreement with experiment than the one-band model for the specific heat γ in the normal state of MgB_2.[21] In comparison, the experimental specific heat γ in the normal state of ZrB_2 is lower than the calculated value.[12,41] Recent highly accurate band-structure and Fermi-surface calculations have implied that superconductivity is unlikely in ZrB_2.[13] Since our single-crystal samples also do not show superconductivity, we believe that the crossover from two dimensionality in MgB_2 to three-dimensional Fermi surfaces in ZrB_2 (Ref. 13) suppresses superconductivity in ZrB_2. The T_c of 5.5 K reported recently[22] then most probably arises from nonstoichiometry. The calculations for MgB_2 (Ref. 13) also indicate that small shifts of $\sim$0.24 eV for the B $2p_\sigma$ bands relative to the $2p_\pi$ bands are necessary to make consistency with experimental Fermi surfaces of MgB_2. It would be important to study ARPES with very high resolution in order to understand the electron-phonon coupling, renormalization of the electronic states, and the origin of multiple gaps. In fact, recent *ab initio* calculations do show that a multiple gap behavior due to anisotropic electron-phonon coupling is valid for MgB_2.[42]

In conclusion, a comparative study of the electronic structure of MgB_2 and ZrB_2 is reported. The B $1s$ core levels in high quality MgB_2 and ZrB_2 exhibit a typical metallic boride peak. The Mg $2p$ core level also is a single peak with negligible intensity in charge-transfer satellites, in contrast to cluster calculations. The bulk plasmon satellite in MgB_2 is observed about 22 eV above the main peak in the B $1s$ and Mg $2p$ core levels. The valence bands are consistent with band-structure calculations, indicating a much higher DOS at E_F for MgB_2 compared to ZrB_2. The high T_c in MgB_2 is due to p-derived DOS while d DOS at E_F dominates the properties in ZrB_2.

A.C. thanks Professor D. D. Sarma for very valuable discussions.

*Email address: chetanjari@yahoo.com

[1] J. Nagamatsu, N. Nakagawa, T. Muranaka, Y. Zenitani, and J. Akimitsu, Nature (London) **410**, 63 (2001).
[2] W.L. McMillan, Phys. Rev. **167**, 331 (1968).
[3] P.B. Allen and R.C. Dynes, Phys. Rev. B **12**, 905 (1975).
[4] J.E. Hirsch, Phys. Lett. A **282**, 392 (2001); M. Imada, J. Phys. Soc. Jpn. **70**, 1218 (2001).
[5] For a review, see, C. Buzea and T. Yamashita, Supercond. Sci. Technol. **14**, R115 (2001).
[6] X.L. Chen, Q.Y. Tu, L. Dai, and Y.P. Xu, Mod. Phys. Lett. B **16**, 73 (2002).
[7] S.L. Bud'ko, G. Lapertot, C. Petrovic, C.E. Cunningham, N. Anderson, and P.C. Canfield, Phys. Rev. Lett. **86**, 1877 (2001).
[8] H. Kotegawa, K. Ishida, Y. Kitaoka, T. Muranaka, and J. Akimitsu, Phys. Rev. Lett. **87**, 127001 (2001).
[9] R. Osborn, E.A. Goremychkin, A.I. Kolesnikov, and D.G. Hinks, Phys. Rev. Lett. **87**, 017005 (2001).
[10] J.M. An and W.E. Pickett, Phys. Rev. Lett. **86**, 4366 (2001).
[11] J. Kortus, I.I. Mazin, K.D. Belashchenko, V.P. Antropov, and L.L. Boyer, Phys. Rev. Lett. **86**, 4656 (2001).
[12] I.R. Shein and A.L. Ivanovskii, Phys. Solid State **44**, 1833 (2002).
[13] H. Rosner, J.M. An, W.E. Pickett, and S.-L. Drechsler, Phys. Rev. B **66**, 024521 (2002).
[14] P.P. Singh, Phys. Rev. Lett. **87**, 087004 (2001).
[15] H. Uchiyama, K.M. Shen, S. Lee, A. Damascelli, D.H. Lu, D.L. Feng, Z.-X. Shen, and S. Tajima, Phys. Rev. Lett. **88**, 157002 (2002).
[16] R. Jin, M. Paranthanam, H.Y. Zhai, H.M. Christen, D.K. Christen, and D. Mandrus, Phys. Rev. B **64**, 220506 (2001); W.N. Kang, C.U. Jung, K.H.P. Kim, M-S. Park, S.Y. Lee, H.-J. Kim, E-M. Choi, K.M. Kim, M-S. Kim, and S.-I. Lee, Appl. Phys. Lett. **79**, 982 (2001).
[17] F. Giubileo, D. Roditchev, W. Sacks, R. Lamy, D.X. Thanh, J. Klein, S. Miraglia, D. Fruchart, J. Marcus, and Ph. Monod, Phys. Rev. Lett. **87**, 177008 (2001).
[18] S. Tsuda, T. Yokoya, T. Kiss, Y. Takano, K. Togano, H. Kito, H. Ihara, and S. Shin, Phys. Rev. Lett. **87**, 177006 (2001).
[19] F. Bouquet, Y. Wang, I. Sheikin, T. Plackowski, A. Junod, S. Lee, and S. Tajima, Phys. Rev. Lett. **89**, 257001 (2002).
[20] A.Y. Liu, I.I. Mazin, and J. Kortus, Phys. Rev. Lett. **87**, 087005 (2001).
[21] A.A. Golubov, J. Kortus, O.V. Dolgov, O. Jepsen, Y. Kong, O.K. Anderson, B.J. Gibson, K. Ahn, and R.K. Kremer, J. Phys.: Condens. Matter **14**, 1353 (2002).
[22] V.A. Gasparov, N.S. Sidorov, I.I. Zverkova, and M.P. Kulakov, JETP Lett. **73**, 532 (2001).
[23] D. Kaczorowski, A.J. Zaleski, O.J. Zogal, and J. Klamut, cond-mat/0103571 (unpublished).
[24] R.P. Vasquez, C.U. Jung, M.-S. Park, H.-J. Kim, J.Y. Kim, and S.-I. Lee, Phys. Rev. B **64**, 052510 (2001).
[25] K. Ueda, H. Yamamoto, and M. Naito, Physica C **378-381**, 225 (2002).
[26] N.V. Dobrodey, A.I. Streltsov, L.S. Cederbaum, C. Villani, and F. Tarantelli, Phys. Rev. B **66**, 165103 (2002).
[27] A. Goldoni, R. Larciprete, S. Lizzit, S. La Rosa, A. Bianco, and M. Bertolo, Phys. Rev. B **66**, 132503 (2002).
[28] V.P. Zhukov, V.M. Silkin, E.V. Chulkov, and P.M. Echenique, Phys. Rev. B **66**, 132503 (2002).
[29] Y. Takano, H. Takeya, H. Fujii, H. Kumakura, T. Hatano, K. Togano, H. Kito, and H. Ihara, Appl. Phys. Lett. **78**, 2914 (2001); S. Otani and Y. Ishizawa, J. Cryst. Growth **165**, 319 (1996); T. Mori and S. Otani (unpublished).
[30] S. Hofmann and M.G. Stepanova, Appl. Surf. Sci. **90**, 227 (1995).
[31] S.A. Schwarz and C.R. Helms, J. Vac. Sci. Technol. **16**, 781 (1979).
[32] J. Naumann, J. Osing, A.J. Quinn, and I.V. Shvets, Surf. Sci. **388**, 212 (1997).
[33] O.R. de la Fuente, M.A. Gonzalez, and J.M. Rojo, Phys. Rev. B **63**, 085420 (2001).
[34] P. Reinke, G. Francz, and P. Oelhafen, Thin Solid Films **290-291**, 148 (1996).
[35] S. Valeri, G.C. Gazzadi, A. Rota, and A. di Bona, Surf. Sci. **120**, 323 (1997).
[36] C.R. Eddy, Jr. and B. Molnar, J. Electron. Mater. **28**, 314 (1999).
[37] Y. Zhu, A.R. Moodenbaugh, G. Schneider, J.W. Davenport, T. Vogt, Q. Li, G. Gu, D.A. Fischer, and J. Tafto, Phys. Rev. Lett. **88**, 247002 (2002).
[38] J.J. Yeh and I. Lindau, At. Data Nucl. Data Tables **32**, 1 (1985).
[39] T.A. Callcott, L. Lin, G.T. Woods, G.P. Zhang, J. R. Thompson, M. Paranthanam and D.L. Ederer, Phys. Rev. B **64**, 132504 (2001); E.Z. Kurmaev, I.I. Lyakhovskaya, J. Kortus, N. Miyata, M. Demeter, M. Neymann, M. Yanagihara, M. Watanabe, T. Muranaka, and J. Akimitsu, *ibid.* **65**, 134509 (2002); J. Nakamura, M. Watanabe, T. Oguchi, S. Nasubida, E. Kabasawa, N. Yamada, K. Kuroki, H. Yamazaki, S. Shin, Y. Umeda, S. Minakawa, N. Kimura, and H. Aoki, J. Phys. Soc. Jpn. **71**, 408 (2002).
[40] H. Ihara, M. Hirabayashi, and H. Nakagawa, Phys. Rev. B **16**, 726 (1977).
[41] Y.S. Tyan, L.E. Toth, and Y.A. Chang, J. Phys. Chem. Solids **30**, 785 (1969).
[42] H.J. Choi, D. Roundy, H. Sun, M.L. Cohen, and S.G. Louie, Nature (London) **418**, 758 (2002).